

SCIENTIFIC REPORTS



OPEN

Production of three phenylethanoids, tyrosol, hydroxytyrosol, and salidroside, using plant genes expressing in *Escherichia coli*

Daeun Chung, So Yeon Kim & Joong-Hoon Ahn

Polyphenols, which include phenolic acids, flavonoids, stilbenes, and phenylethanoids, are generally known as useful antioxidants. Tyrosol, hydroxytyrosol, and salidroside are typical phenylethanoids. Phenylethanoids are found in plants such as olive, green tea, and *Rhodiola* and have various biological activities, including the prevention of cardiovascular diseases, cancer, and brain damage. We used *Escherichia coli* to synthesize three phenylethanoids, tyrosol, hydroxytyrosol, and salidroside. To synthesize tyrosol, the aromatic aldehyde synthase (AAS) was expressed in *E. coli*. Hydroxytyrosol was synthesized using *E. coli* harboring AAS and *HpaBC*, which encodes hydroxylase. In order to synthesize salidroside, 12 uridine diphosphate-dependent glycosyltransferases (UGTs) were screened and UGT85A1 was found to convert tyrosol to salidroside. Using *E. coli* harboring AAS and UGT85A1, salidroside was synthesized. Through the optimization of these three *E. coli* strains, we were able to synthesize 531 mg/L tyrosol, 208 mg/L hydroxytyrosol, and 288 mg/L salidroside, respectively.

Many countries have traditional foods or medicines; olive oil in southern Europe and the Middle East and green tea from Asia are considered regional traditional foods. Olive oil and green tea contain many antioxidants due to presence of phenolic compounds. Antioxidant protects cells and tissues from oxidative injury¹, which can cause Parkinson's disease, Alzheimer's disease, other forms of dementia, cancer, and heart disease. Historically, olive oil has been called a "miracle food" because it aids in digestion and combats skin cancer. Also, olive oil has been shown to effect on cardiovascular disease and certain types of cancers². Two major ingredients in olive are tyrosol and hydroxytyrosol, both of which are considered bioactive ingredients having various biological activities. It has been proven that tyrosol can lower the risk of developing Alzheimer's disease³. Salidroside, a glucoside of tyrosol, is one of the major ingredients of the medicinal herb, *Rhodiola*⁴. Salidroside exhibits various biological activities, including nerve and brain cell protection, bone loss reduction and weight reduction⁵⁻⁸. Tyrosol, hydroxytyrosol, and salidroside belong to a group of plant phenolic compounds called phenylethanoids.

Tyrosol is synthesized from tyrosine. There are two possible biosynthesis pathways for tyrosol synthesis in plants. In the first proposed pathway, tyrosine is converted into tyramine by tyrosine decarboxylase (TDC). Subsequent oxidation and reduction of tyramine result in the formation of tyrosol⁹ (Fig. 1). However, growing evidence indicates that tyrosol is synthesized via tyramine, as TDC was identified in *Rhodiola sachalinensis*^{10,11}. The carbon backbone of tyrosol is C6-C2. Plant phenolic compounds have been synthesized via cinnamic acid, which has a C6-C3 carbon backbone and is derived from phenylalanine. In order to synthesize other phenolic compounds such as flavonoids and stilbenes, malonyl-CoA serves as a carbon donor to transfer two carbons to hydroxycinnamic acid. The synthesis of C6-C1 phenolic compounds, such as benzoic acid relies on the coenzyme A-dependent β -oxidation of cinnamoyl-CoA¹¹. These results support that tyrosol is synthesized through tyrosine decarboxylation.

Department of Integrative Bioscience and Biotechnology, Bio/Molecular Informatics Center, Konkuk University, Seoul, 05029, Republic of Korea. Daeun Chung and So Yeon Kim contributed equally to this work. Correspondence and requests for materials should be addressed to J.-H.A. (email: jhahn@konkuk.ac.kr)

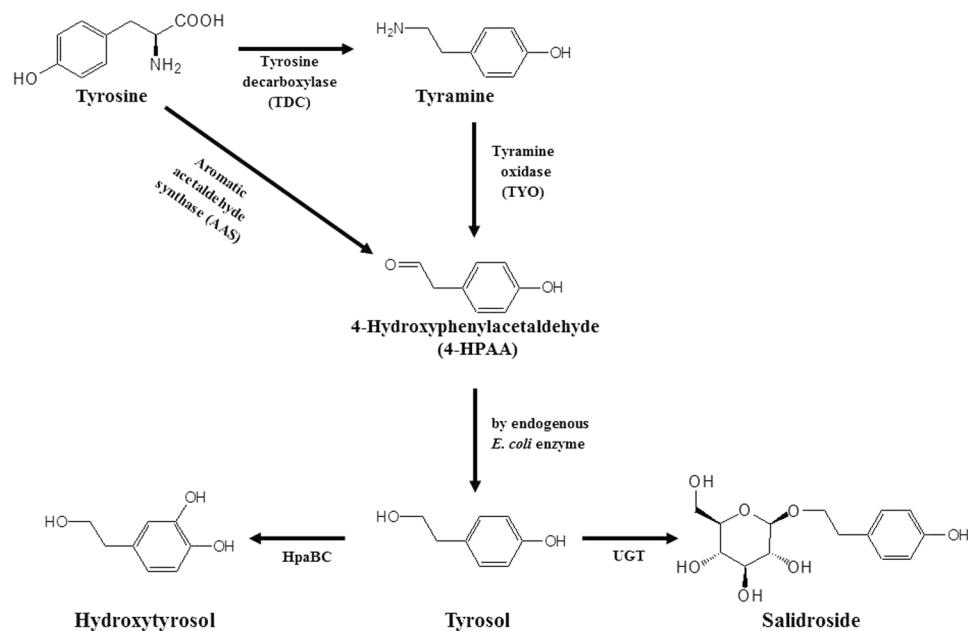


Figure 1. Scheme of biosynthesis of three phenylethanoids, tyrosol, hydroxytyrosol, and salidroside.

Salidroside is synthesized from tyrosol by a uridine diphosphate dependent glycosyltransferase (UGT). UGT73B6 from *R. sachalinensis* was found to be involved in the biosynthesis of salidroside although it also produces icaricide D2 using tyrosol^{12,13}.

Escherichia coli has been widely used to synthesize diverse phytochemicals. Biological synthesis using microorganisms has advantages over enzymatic and chemical syntheses; it does not require expensive cofactors and it confers regioselectivity and stereoselectivity. Tyrosol, hydroxytyrosol, and salidroside have been previously synthesized in *E. coli*. There are two possible routes for the production of tyrosol in *E. coli*. In the first method using tyrosine as a substrate, TDC and TYO were introduced into an *E. coli feaB* (phenylacetaldehyde dehydrogenase) deletion strain¹⁴. FeaB competes for 4-hydroxyphenylacetaldehyde (4-HPAA) and produces 4-hydroxyphenylacetate instead of tyrosol. Therefore, deletion of *feaB* results in an increase in tyrosol production by approximately 43%. Using this *E. coli* strain, Satoh *et al.*¹⁴ were able to synthesize 69 mg/L tyrosol. Second route of tyrosol production in *E. coli* utilized *aro10* from yeast encoding pyruvate decarboxylase that converts 4-hydroxyphenylpyruvate to 4-HPAA. Bai *et al.*¹³ used *aro10* and other genes for the biosynthesis of tyrosine, in addition to several *E. coli* mutants to produce tyrosol. This group also introduced UGT into the tyrosine producing *E. coli* strain to synthesize salidroside¹³. Hydroxytyrosol was synthesized using tyrosine hydroxylase (TH), L-DOPA decarboxylase (DDC) and tyramine oxidase (TYO)¹⁴.

Studies of plant aromatic amino acid decarboxylases (AAADs) revealed that some AAADs are bifunctional enzymes capable of catalyzing both decarboxylation and oxidation^{15–17}. This family of AAADs is known as aromatic aldehyde synthases (AASs). AAS converts tyrosine into 4-HPAA, and then 4-HPAA can be converted into tyrosol in *E. coli*. In this report, we used plant AAS to synthesize tyrosol, hydroxytyrosol, and salidroside in *E. coli*. Through the metabolic engineering of *E. coli*, 531 mg/L tyrosol and 208 mg/L hydroxytyrosol were synthesized. Furthermore, in order to synthesize salidroside, we screened 12 UGTs from *Arabidopsis thaliana*. Using engineered *E. coli* harboring AAS and the identified UGT, we could synthesize 288 mg/L salidroside.

Results

Synthesis of tyrosol using AAS in *E. coli*. For the synthesis of tyrosol in *E. coli*, we constructed the pathway from tyrosine to tyrosol using AAS. AAS is a bifunctional enzyme that converts tyrosine into 4-HPAA oxidation^{15–17}. In *E. coli*, 4-HPAA is converted to tyrosol by alcohol dehydrogenase(s)¹⁴. We tested three different AAS genes from *A. thaliana*, *Petunia hybrid*, and *Petroselinum crispum*. After induction of each protein, tyrosine (100 μM) was added to the culture. The culture filtrates from the *E. coli* strains harboring each AAS were analyzed using HPLC. *E. coli* harboring AAS from *P. crispum* produced approximately 12.6 mg/L tyrosol (Fig. 2). *E. coli* harboring AAS from *A. thaliana* did not produce tyrosol and *E. coli* harboring AAS from *P. hybrid* produced approximately 5.3 mg/L tyrosol. The structure of the reaction product in Fig. 1 was determined to be tyrosol using NMR. We decided to use the PcAAS for further experiments. We could not observe the reaction intermediates such as 4-HPAA, suggesting that AAS and the endogenous *E. coli* reductase, which converts 4-HPAA into tyrosol, were balanced in the production of tyrosol.

Tyrosol is synthesized from tyrosine. Therefore, it is likely that total tyrosine content is correlated with the final tyrosol yield. The reaction intermediate, the 4-HPAA, can be converted into 4-hydroxyphenylacetic acid by phenylacetaldehyde dehydrogenase (*feaB*), which competes with the *E. coli* alcohol dehydrogenase for 4-HPAA and results in reduction of the final yield of tyrosol. We used two mutants B-TP and B-TPF (Table 1). The strain B-TP produced more tyrosine than did the wild type due to the deletions of the transcriptional regulator, *tyrR*, which

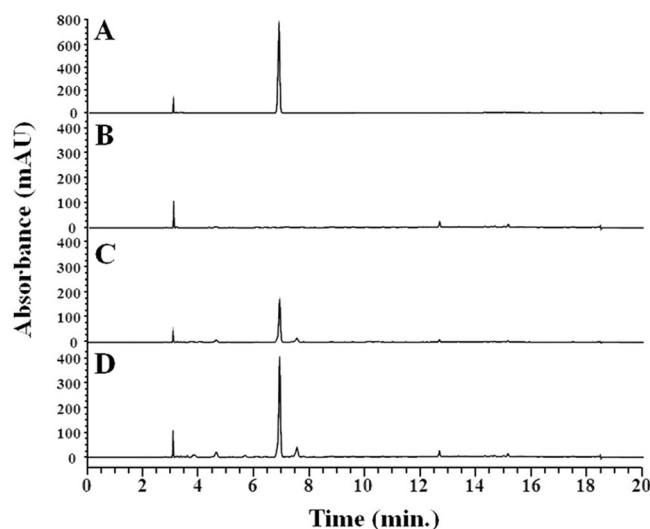


Figure 2. Production of tyrosol using *E. coli* harboring AAS. (A) standard tyrosol; (B) AAS from *Arabidopsis thaliana*; (C) AAS from *Petunia hybrid*; (D) AAS from *Petroselinum crispum*.

is inhibited by tyrosine, and *pheA* encoding a chorismate mutase/prephenate dehydratase that drives prephenate toward the biosynthesis of the phenylalanine instead of biosynthesis of tyrosine^{18,19}. The strain B-TPF contains deletions in *feaB*, *tyrR*, and *pheA*. *FeaB* encodes phenylacetaldehyde dehydrogenase, which converts 4-HPAA to 4-hydroxyphenylacetate (4-HPA). Deletion of this gene was expected to increase more 4-HPAA for tyrosol synthesis. As an alternative route for the tyrosol biosynthesis, we used tyrosine decarboxylase (*TDC*) from *Papaver somniferum* and tyrosine oxidase (*TYO*) from *Micrococcus luteus*. These two genes were transformed into *E. coli* BL21(DE3). Strain B-TY1 produced 138.9 mg/L of tyrosol, B-TY2 produced 188.1 mg/L, and B-TY3 produced 250.4 mg/L (Fig. 3). This result demonstrated that the contents of tyrosine and 4-HPAA are critical to the final yield of tyrosol. However, B-TY4, which had *TDC* and *TYO*, produced only 49.2 mg/L tyrosol.

Strain B-TY3 was used to synthesize tyrosol. The optimal culturing temperature and the initial cell concentration were determined. Tyrosol production at 30 °C in B-TY3 was better than that at 25 °C or 37 °C. The production at 25 °C and 37 °C was 57.7% and 20.4% of that at 30 °C, respectively. The initial cell concentration was tested at OD₆₀₀ = 0.5, 1, 1.5, 2, 2.5, and 3. The production of tyrosol at OD₆₀₀ = 0.5 was highest, and production declined with increasing cell concentrations. Using the optimized incubation time and cell concentration of B-TY3, the production of tyrosol was monitored for 48 h. The production of tyrosol continued to increase until 36 h, at which 539.4 mg/L tyrosol was produced (Fig. 4). After 36 h, tyrosol production did not increase.

Synthesis of salidroside in *E. coli*. We attempted to synthesize salidroside in *E. coli*. Salidroside is 2-(4-hydroxyphenyl) ethyl β-D-glucopyranoside. In order to synthesize salidroside from tyrosol, a uridine-dependent glycosyltransferase (UGT), which transfers glucose from UDP-glucose to an acceptor molecule such as tyrosol, was needed. We screened 12 UGTs from *A. thaliana* to identify a UGT that synthesizes salidroside from tyrosol. These 12 UGTs are known to transfer a glucose group from UDP-glucose to small compounds such as hydroxycinnamates like *p*-coumaric acid, caffeic acid, and ferulic acid^{20–23} and monoterpenoids like geraniol and perillyl alcohol²⁴. We transformed *E. coli* with each UGT and each transformant was supplemented with tyrosol. *E. coli* strains harboring *AtUGT73C5*, *AtUGT73C6*, or *AtUGT85A1*, yielded a product that had the same retention time as a standard of salidroside (Fig. 1S). Among these, *AtUGT85A1* produced more salidroside than did the others. Therefore, we used *AtUGT85A1* for salidroside synthesis.

To synthesize salidroside from glucose, we transformed *E. coli* with both *PcAAS* and *AtUGT84A1*. The resulting transformant, B-SAL1, was used for the production of salidroside. The analysis of the B-SAL1 culture filtrate using HPLC revealed a peak with the same retention time as salidroside (Fig. 5). The tyrosol was not observed, indicating that tyrosol was converted into salidroside as soon as it was produced. The structure of the reaction product was determined to be salidroside by NMR.

The synthesis of tyrosol was higher in strain B-TPF. We used B-TPF to synthesize salidroside. The wild type strain (B-SAL1 in Table 1) produced approximately 54.8 mg/L salidroside while the B-TPF strain (B-SAL2 in Table 1) produced 165.8 mg/L, approximately 3-fold more. The optimized reaction time and the initial cell concentration using B-SAL2 were determined to be 25 °C at OD₆₀₀ = 5. Using the optimized incubation temperature and cell concentration, the synthesis of salidroside using B-SAL2 was monitored. Until 8.5 h, both tyrosol and salidroside had accumulated, and after which, the accumulation of salidroside continued to increase until 48 h, at which approximately 287.9 mg/L salidroside was synthesized (Fig. 6). But, tyrosol was converted into salidroside immediately after it was formed. Tyrosol was not observed at the end of the reaction.

Synthesis of hydroxytyrosol in *E. coli*. Hydroxytyrosol can also be synthesized from tyrosol by hydroxylation. We tested the *HpaBC* gene, encoding 4-hydroxyphenylacetate 3-hydroxylase, from *E. coli*²⁵ and *Sam5* from

Plasmids or <i>E. coli</i> strain or Primers	Relevant properties or genetic marker	Source or reference
Plasmids		
pACYCDDuet	P15A ori, Cm ^r	Novagen
pCDFDuet	CloDE13 ori, Str ^r	Novagen
pGEX	f1 ori, Amp ^r	GE Healthcare
Constructs		
pC-PcAAS	pCDFDuet carrying aromatic aldehyde synthase (AAS) from <i>Petroselinum crispum</i>	This study
pC-PcAAS-HpaBC	pCDFDuet carrying aromatic aldehyde synthase (AAS) from and <i>P. crispum</i> and <i>HpaBC</i> from <i>Escherichia coli</i>	This study
pE-HpaBC	pETDuet carrying <i>HpaBC</i> from <i>E. coli</i>	This study
pC-TDC-TYO	pCDFDuet carrying TDC from <i>Papaver somniferum</i> and TYO from <i>Micrococcus luteus</i>	This study
Strains		
BL21 (DE3)	F ^{- ompT hsdS_B(r_B⁻ m_B⁻) gal dcm lon}	(DE3) Novagen
B-TP	BL21(DE3) Δ tyrR::FRT- Δ PheA::FRT-kan ^R -FRT	36
B-TPF	BL21(DE3) Δ tyrR::FRT- Δ PheA:: Δ feaB-FRT FRT-kan ^R -FRT	This study
B-TY1	BL21 (DE3) harboring pC-PcAAS	This study
B-TY2	B-TP harboring pC-PcAAS	This study
B-TY3	B-TPF harboring pC-PcAAS	This study
B-TY4	BL21 (DE3) harboring pC-TDC-TYO	This study
B-SAL1	BL21 (DE3) harboring pC-PcAAS and pG-AtUGT85A1	This study
B-SAL2	B-TPF harboring pC-PcAAS and pG-AtUGT85A1	This study
B-HTY1	BL21 (DE3) harboring pC-PcAAS-HpaBC	This study
B-HTY2	BL21 (DE3) harboring pC-PcAAS and pE-HpaBC	This study
B-HTY3	B-TPF harboring pC-PcAAS-HpaBC	This study

Table 1. Plasmids, *Escherichia coli* strains, and primers used in this study.

*Saccharothrix espanaensis*²⁶ in order to convert tyrosol into hydroxytyrosol. *HpaBC* and *Sam5* were used to modify other phenolic compounds such as *p*-coumaric acid, tyrosine, and flavonoids^{27–29}. The *HpaBC* or *Sam5* genes were coexpressed with *PcAAS* in *E. coli*, and each transformant was tested for the production of hydroxytyrosol. The transformant harboring *HpaBC* and *PcAAS* produced more hydroxytyrosol than that harboring both *Sam5* and *PcAAS* (data not shown). Therefore, we used *HpaBC* for the synthesis of hydroxytyrosol.

We made two constructs and independently transformed them into *E. coli*, independently. The strain B-HTY1 harbored a single construct containing both *PcAAS* and *HpaBC* and the strain B-HTY2 harbored two separate constructs, one with *PcAAS* and the other with *HpaBC*. We compared the production of hydroxytyrosol. HPLC analysis of culture filtrates from both strains revealed a new peak which had a different retention time with tyrosol. NMR analysis of this peak revealed that the reaction product was hydroxytyrosol. B-HTY1 produced 80.3 mg/L of hydroxytyrosol but B-HTY2 produced only 16.6 mg/L, indicating that the strain harboring the single construct produced more tyrosol.

We used strain B-TPF to produce hydroxytyrosol because this strain produced more tyrosol than *E. coli* BL21(DE3). The strain B-HTY3 produced 116.7 mg/L tyrosol, more than B-HTY1 (80.3 mg/L) did. Using B-HTY3, the optimized initial cell concentration and the incubation temperature were determined to be OD₆₀₀ = 1.0 and 25 °C, respectively. Using the optimized cell concentration and the incubation time, we monitored the production of hydroxytyrosol. As shown in Fig. 7, production of hydroxytyrosol was initially observed after 3 h, and production continued to increase until 30 h, after which 208 mg/L hydroxytyrosol was synthesized. Tyrosol was observed until 5 h at less than 5 mg/L, indicating that tyrosol was converted into hydroxytyrosol as soon as it was produced.

Discussion

Tyrosol has been synthesized in *E. coli* using *TDC* and *TYO*¹⁴ or using *Aro10* from yeast¹³. Hydroxytyrosol was also synthesized using *TH*, *DDC* and *TYO*³⁰ and salidroside was synthesized using *Aro10* and *UGT73B6*¹². The protein encoded by *Aro10* uses 4-hydroxypyruvate as a substrate to synthesize 4-HPAA, which undergoes further reduction to make tyrosol. *Aro10* does not use tyrosine but 4-hydroxypyruvate as an intermediate for the synthesis of tyrosine. Therefore, they not only used *E. coli* mutants but also overexpressed several genes of the shikimate pathway of *E. coli*. AAS, which exhibits both tyrosine decarboxylase and deaminase activity, converts tyrosine into 4-HPAA and then the endogenous *E. coli* reductase converts it into tyrosol. AAS replaces the activity of both *TDC* and *TYO*, and is therefore, an efficient way to synthesize tyrosol from tyrosine in *E. coli*. This is the first report that AAS from plants could synthesize tyrosol as well as hydroxytyrosol and salidroside. We were able to synthesize 531 mg/L tyrosol without overexpressing other genes to increase the content of tyrosine in the cell.

For the synthesis of salidroside, the selection of UGT was critical. We screened 12 UGTs from *A. thaliana* and found AtUGT85A1 as the best UGT for the synthesis of salidroside. AtUGT85A1 is involved in the regulation of the plant hormone trans-zeatin through *O*-glucosylation³¹. It was surprising that AtUGT85A1 also could

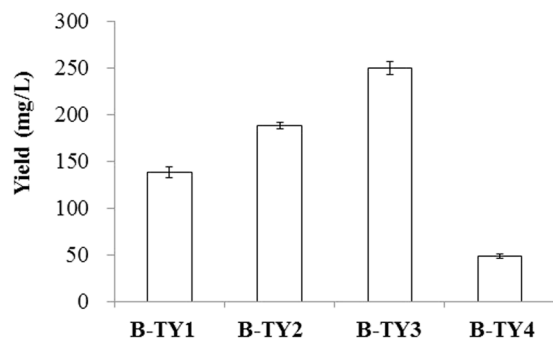


Figure 3. Effect of different *E. coli* strain on the production of tyrosol. B-TY1, wild type harboring AAS; B-TY2, *tyrR* and *pheA* deletion mutant harboring AAS; B-TY3, *tyrR*, *pheA*, and *feaB* deletion mutant harboring AAS; B-TY4, wild type harboring TDC and TYO.

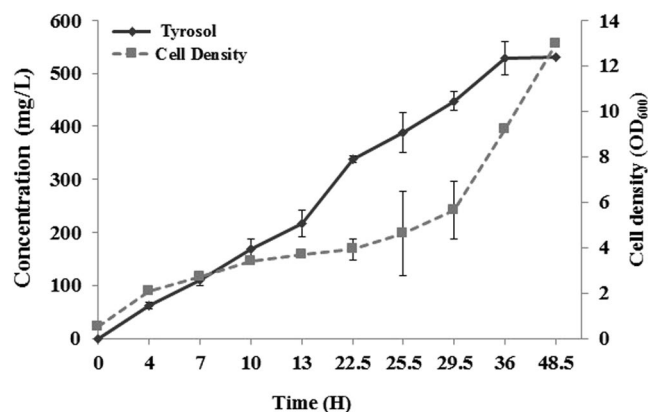


Figure 4. Production of tyrosol using strain B-TY3 after optimization of incubation time and cell concentration.

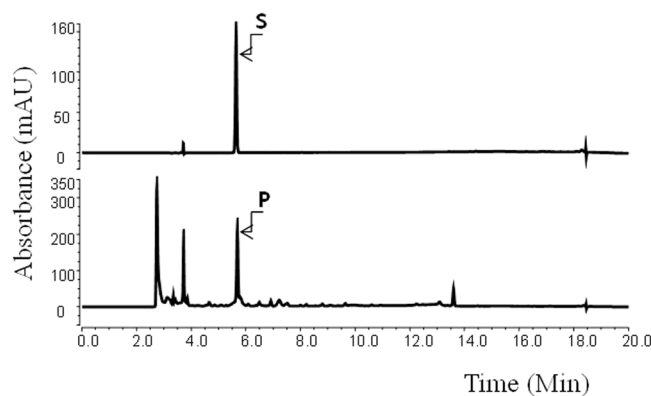


Figure 5. Production of salidoside using strain B-SAL1. S, standard salidoside; P, reaction product.

glucosylate tyrosol to salidoside. Some plant UGTs exhibited substrate promiscuity³². Therefore, AtUGT85A1 was capable of utilize diverse sugar acceptors including trans-zeatin, tyrosol, hydroxytyrosol, and 4-hydroxy benzoic acid (data not shown). However, unlike UGT73B6 from *Rhodiola*¹³, which was previously used for the synthesis of salidoside, AtUGT85A1 exhibited regioselectivity; it did not transfer glucose to the phenolic hydroxyl group to produce icariside. Therefore, the final yield of salidoside was 288 mg/L, which was much higher than that of previous report¹².

We synthesized tyrosol using *E. coli* harboring TDC and TYO and compared the final yield to that of *E. coli* harboring AAS. The yield of tyrosol using TDC and TYO (49.2 mg/L) was lower than that using AAS (138.9 mg/L). Therefore, we used AAS gene to synthesize tyrosol. When hydroxytyrosol was fed to *E. coli* harboring AtUGT85A1, most of hydroxytyrosol was converted into hydroxysalidoside. This indicated that AtUGT85A1

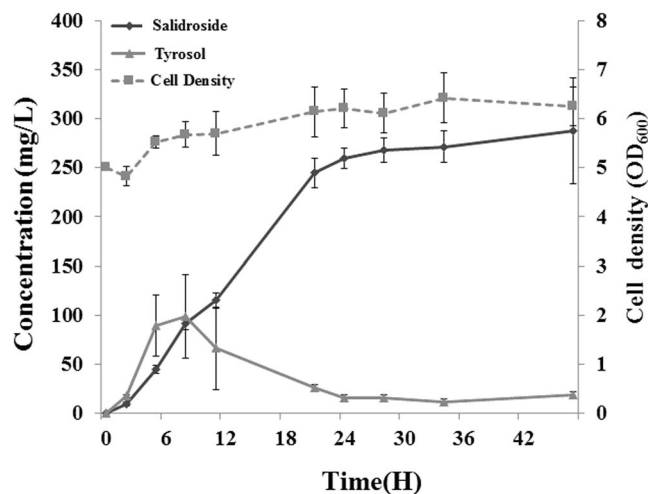


Figure 6. Production of salidroside using strain B-SAL2 after optimization of incubation time and cell concentration.

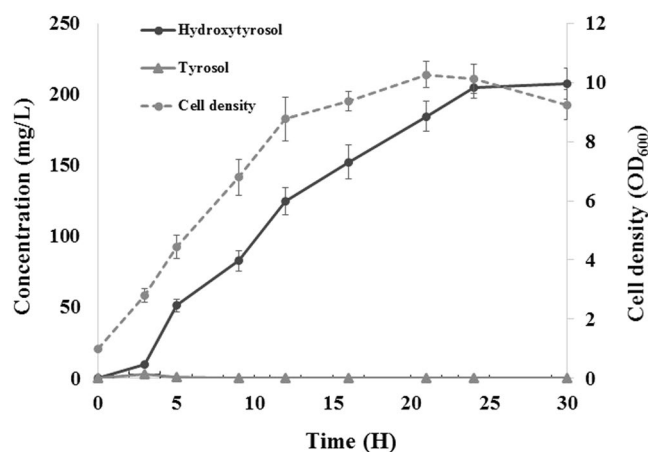


Figure 7. Production of hydroxytyrosol using strain B-THY3 after optimization of incubation time and cell concentration.

could use hydroxytyrosol as a substrate. However, when hydroxysalidroside was synthesized using B-HTY3 harboring *AtUGT85A1*, only a small amount of hydroxysalidroside was synthesized and more hydroxytyrosol remained. Taken together, it appears that the reaction intermediate(s) inhibits the glycosyltransferase reaction. In particular, the byproduct from the reaction of oxygenase (during salidroside synthesis: TYO; during hydroxysalidroside synthesis: HpaBC) appears to inhibit the UGT activity. On the other hand, production of salidroside using Aro10 and UGT73B6 yielded only 56.9 mg/L salidroside while 764.6 mg/L tyrosol remained¹³. Therefore, selection of UGT having high activity as well as the presence of a UGT inhibitor, was critical to the final yield of salidroside.

Materials and Methods

Constructs and *E. coli* strains. The AAS genes from *A. thaliana*, *P. hybrid*, and *P. crispum* were cloned using reverse transcription polymerase chain reaction (RT-PCR). RNA was isolated from parsley purchased from a local market using the Plant Total RNA Isolation Kit (Qiagen, Velno, Netherlands). cDNA was synthesized as previously described before³³. Primers for cloning AAS were synthesized based on the published parsley AAS sequence (GenBank accession number: M96070.1): 5'-ATGGATCCGATGGGCTCCATCGATAATCTT-3' (BamHI site is underlined.) and 5'-ATGCGGCCGCTTATGATAATACTTCCACGA-3' (NotI site is underlined.); *A. thaliana* AAS gene (AT2G20340.1) 5'-ATGGATCCGATGGAAAATGGAAGCGGGAAG-3' (BamHI site is underlined.) and 5'-ATGCGGCCGCTTACTTGTGAAGCAAGTAAG-3' (NotI site is underlined.); *P. hybrid* AAS gene (GenBank accession number: DQ243784.1) 5'-ATGAATTCGATGGATACTATCAAAATCAACCCA-3' (EcoRI site is underlined.) and 5'-ATGCGGCCGCTTACGCATTCAGCATCATAGTT-3' (NotI site is underlined.). Each AAS gene was subcloned into the corresponding sites of the pCDF-Duet1 vector.

Tyrosine decarboxylase (TDC from *Papaver somniferum*; GenBank U08598.1), and tyrosine oxidase (TYO from *Micrococcus luteus*; GenBank AB010716.1) were synthesized after codon optimization using the published

nucleotide sequences (Figs 2S and 3S). TDC was subcloned into BamHI/HindIII site of pCDF-Duet1 vector, and the resulting construct was pC-TDC. TYO was introduced into the second cloning site (NdeI/XhoI) of pC-TDC and the resulting constructs was called pC-TDC-TYO.

Twelve UGTs (AtUGT71C1 [At2g29750], AtUGT71C2 [At2g29740], AtUGT72B1 [At4g01070], AtUGT72E2 [At5g66690], AtUGT73C1 [At2g36750], AtUGT73C3 [At2g36780], AtUGT73C5 [At2g36800], AtUGT73C6 [At2g36790], AtUGT76D1 [At2g26480], AtUGT76E2 [At5g59590], AtUGT76E12 [At3g46660], AtUGT85A1 [At1g22400]) from *A. thaliana* were subcloned into the pGEX 5X-3 vector.

The list of constructs and *E. coli* strains used in this study can be found in Table 1.

Production of tyrosol, hydroxytyrosol, and salidroside in *E. coli*. For the synthesis of tyrosol, hydroxytyrosol, and salidroside, *E. coli* was grown in LB medium containing 50 µg/mL appropriate antibiotics at 37 °C for 18 hr. The seed culture was inoculated into a fresh LB medium containing antibiotics and incubated at 37 °C until OD₆₀₀ = 1.0. Cells were harvested by centrifugation, washed once with M9 medium. For the initial screening of AAS gene, the cell was resuspended with M9 containing 2% glucose, 50 µg/mL antibiotics, 1 mM IPTG, and 100 µM. For the synthesis of tyrosol, hydroxytyrosol, and salidroside, cells were resuspended with M9 containing 2% glucose, 50 µg/mL antibiotics, 1 mM IPTG, and 0.1% yeast extract. The cell density was adjusted to OD₆₀₀ = 1.0. The resulting culture was incubated at 30 °C for 24 h. To detect tyrosol and hydroxytyrosol production, the culture was extracted with ethylacetate and the organic layer was collected after centrifugation and evaporated to dryness. The remaining reaction product was dissolved with dimethyl sulfoxide (DMSO) and analyzed by Thermo high performance liquid chromatography (HPLC). To examine the production of salidroside, the culture was boiled for 3 min and then centrifuged. The supernatant was filtered using 0.45 µm syringe filter (Millipore, Billerica, MA, USA) and analyzed by HPLC.

To analyze the formation of tyrosol, hydroxytyrosol, and salidroside by HPLC, the mobile phase was composed of water (solution A) and acetonitrile (solution B), which were combined with 0.1% formic acid. The elution program was as follows: the proportion of solution B was gradually increased from 10% to 40% over 8 min, increased to 90% over 4 min, and then maintained over 3 min. Finally, the proportion of solution B was rapidly decreased to 10% and maintained at that composition for 5 min. The flow rate was 1 ml/min.

The structure of reaction product was determined using nuclear magnetic resonance (NMR) spectroscopy^{34,35} (NMR spectra was provided in the Figs 4S, 5S, and 6S). The NMR data were as follows; Tyrosol, ¹H NMR (400 MHz, CDCl₃): δ 7.10 (d, *J* = 8.3 Hz, 2H), 6.78 (d, *J* = 8.3 Hz, 2H), 3.83 (t, *J* = 6.5 Hz, 2H), 2.80 (t, *J* = 6.5 Hz, 2H).

Salidroside, ¹H NMR (400 MHz, DMSO-*d*₆) δ 7.04 (d, *J* = 8.3 Hz, 2H), 6.67 (d, *J* = 8.3 Hz, 2H), 4.17 (d, *J* = 8.5 Hz, 1H), 3.87 (dd, *J* = 16.0, 8.6 Hz, 1H), 3.67 (d, *J* = 11.4 Hz, 1H), 3.56 (dd, *J* = 16.0, 8.8 Hz, 1H), 3.44 (dd, *J* = 11.4, 5.4 Hz, 1H), 3.15 (t, *J* = 8.5 Hz, 1H), 3.07 (m, 1H), 3.06 (d, *J* = 8.5 Hz, 1H), 2.96 (t, *J* = 8.5 Hz, 1H), 2.73 (m, 2H); ¹³C NMR (100 MHz, DMSO-*d*₆) δ 155.6, 129.7, 128.6, 115.0, 102.8, 76.8, 76.7, 73.4, 70.0, 69.9, 61.0, 34.8.

Hydroxytyrosol, ¹H NMR (400 MHz, MeOD): δ 6.68 (d, *J* = 8.0 Hz, 1H), 6.66 (d, *J* = 1.9 Hz, 1H), 6.53 (dd, *J* = 8.0, 2.0 Hz, 1H), 3.68 (t, *J* = 7.2 Hz, 2H), 2.66 (t, *J* = 7.2 Hz, 2H).

References

- Uttara, B., Singh, A. V., Zamboni, P. & Mahajan, R. T. Oxidative stress and neurodegenerative diseases: A review of upstream and downstream antioxidant therapeutic options. *Curr. Neuropharmacol.* **7**, 65–74, doi:10.2174/157015909787602823 (2009).
- Stark, A. H. & Madar, Z. Olive oil as a functional food: epidemiology and nutritional approaches. *Nutr. Rev.* **60**, 170–176, doi:10.1301/002966402320243250 (2002).
- St-Laurent-Thibault, C., Arseneault, M., Longpré, F. & Ramassamy, C. Tyrosol and hydroxytyrosol, two main components of olive oil, protect N2a cells against amyloid-β-induced toxicity. Involvement of the NF-κB signaling. *Curr. Alzheimer. Res.* **8**, 543–551, doi:10.2174/156720511796391845 (2011).
- Yousef, G. G. *et al.* Comparative phytochemical characterization of three *Rhodiola* species. *Phytochemistry* **67**, 2380–2391, doi:10.1016/j.phytochem.2006.07.026 (2006).
- Cifani, C. *et al.* Effect of salidroside, active principle of *Rhodiola rosea* extract, on binge eating. *Physiol. Behav.* **101**, 555–562, doi:10.1016/j.physbeh.2010.09.006 (2010).
- Palumbo, D. R., Occhiuto, F., Spadaro, F. & Circosta, C. *Rhodiola rosea* extract protects human cortical neurons against glutamate and hydrogen peroxide-induced cell death through reduction in the accumulation of intracellular calcium. *Phytother. Res.* **26**, 878–883, doi:10.1002/ptr.v26.6 (2012).
- Zhang, L. *et al.* Neuroprotective effects of salidroside against beta-amyloid-induced oxidative stress in SH-SY5Y human neuroblastoma cells. *Neurochem. Int.* **57**, 547–555, doi:10.1016/j.neuint.2010.06.021 (2010).
- Zhang, J. K. *et al.* Protection by salidroside against bone loss via inhibition of oxidative stress and bone-resorbing mediators. *PLoS One* **8**, e57251, doi:10.1371/journal.pone.0057251 (2013).
- Ma, L. Q. *et al.* Effects of overexpression of endogenous phenylalanine ammonia-lyase (PALr1) on accumulation of salidroside in *Rhodiola sachalinensis*. *Plant Biol. (Stuttg)* **10**, 323–333, doi:10.1111/j.1438-8677.2007.00024.x (2008).
- Zhang, J. X. *et al.* A tyrosine decarboxylase catalyzes the initial reaction of the salidroside biosynthesis pathway in *Rhodiola sachalinensis*. *Plant Cell Rep* **30**, 1443–1453, doi:10.1007/s00299-011-1053-7 (2011).
- Qualley, A. V. *et al.* Completion of the core β-oxidative pathway of benzoic acid biosynthesis in plants. *Proc. Natl. Acad. Sci. USA* **109**, 16383–16388, doi:10.1073/pnas.1211001109 (2012).
- Ma, L. Q. *et al.* Molecular cloning and overexpression of a novel UDP-glucosyltransferase elevating salidroside levels in *Rhodiola sachalinensis*. *Plant Cell Rep.* **26**, 989–999, doi:10.1007/s00299-007-0317-8 (2007).
- Bai, Y. *et al.* Production of salidroside in metabolically engineered *Escherichia coli*. *Sci. Rep.* **4**, 6640, doi:10.1038/srep06640 (2014).
- Satoh, Y. *et al.* Engineering of a tyrosol-producing pathway, utilizing simple sugar and the central metabolic tyrosine, in *Escherichia coli*. *J. Agric. Food. Chem.* **60**, 979–984, doi:10.1021/jf203256f (2012).
- Kaminaga, Y. *et al.* Plant phenylacetaldehyde synthase is a bifunctional homotetrameric enzyme that catalyzes phenylalanine decarboxylation and oxidation. *J. Biol. Chem.* **281**, 23357–23366, doi:10.1074/jbc.M602708200 (2006).
- Torrens-Spence, M. *et al.* Biochemical evaluation of a parsley tyrosine decarboxylase results in a novel 4-hydroxyphenylacetaldehyde synthase enzyme. *Biochem. Biophys. Res. Commun.* **418**, 211–216, doi:10.1016/j.bbrc.2011.12.124 (2012).
- Torrens-Spence, M. *et al.* Biochemical evaluation of the decarboxylation-deamination activities of plant aromatic amino acid decarboxylase. *J. Biol. Chem.* **288**, 2376–2387, doi:10.1074/jbc.M112.401752 (2013).

18. Lütke-Eversloh, T. & Stephanopoulos, G. L-Tyrosine production by deregulated strains of *Escherichia coli*. *Appl. Microbiol. Biotechnol.* **75**, 103–110, doi:10.1007/s00253-006-0792-9 (2007).
19. Juminaga, D. *et al.* Modular engineering of L-tyrosine production in *Escherichia coli*. *Appl. Environ. Microbiol.* **78**, 89–98, doi:10.1128/AEM.06017-11 (2012).
20. Lim, E. K. *et al.* Identification of glucosyltransferase genes involved in sinapate metabolism and lignin synthesis in *Arabidopsis*. *J. Biol. Chem.* **276**, 4344–4349, doi:10.1074/jbc.M007263200 (2001).
21. Lim, E.-K. *et al.* The activity of *Arabidopsis* glucosyltransferases toward salicylic acid, 4-hydroxybenzoic acid, and benzoates. *J. Biol. Chem.* **277**, 586–592, doi:10.1074/jbc.M109287200 (2002).
22. Lim, E.-K., Higgins, G. S., Li, Y. & Bowles, D. J. Regioselectivity of glucosylation of caffeic acid by a UDP-glucose:glucosyltransferase is maintained in planta. *Biochem. J.* **373**, 987–992, doi:10.1042/bj20021453 (2003).
23. Lim, E.-K., Jackson, R. G. & Bowles, D. J. Identification and characterization of *Arabidopsis* glucosyltransferase capable of glucosylating coniferyl aldehyde and sinapyl aldehyde. *FEBS Letters* **579**, 2802–2806, doi:10.1016/j.febslet.2005.04.016 (2005).
24. Caputi, L., Lim, E.-K. & Bowles, D. J. Discovery of new biocatalysts for the glucosylation of terpenoid scaffolds. *Chem. Eur. J.* **14**, 6656–6662, doi:10.1002/chem.v14:22 (2008).
25. Xu, L. & Sandvik, E. R. Characterization of 4-hydroxyphenylacetate 3-hydroxylase (HpaB) of *Escherichia coli* as a reduced flavin adenine dinucleotide-utilizing monooxygenase. *Appl. Environ. Microbiol.* **66**, 481–486, doi:10.1128/AEM.66.2.481-486.2000 (2000).
26. Berner, M. *et al.* Genes and enzymes involved in caffeic acid biosynthesis in the actinomycete *Saccharothrix espanaensis*. *J. Bacteriol.* **188**, 2666–2673, doi:10.1128/JB.188.7.2666-2673.2006 (2006).
27. Lin, Y. & Yan, Y. Biosynthesis of caffeic acid in *Escherichia coli* using its endogenous hydroxylase complex. *Microbiol. Cell Fact.* **11**, 42, doi:10.1186/1475-2859-11-42 (2012).
28. Lee, H., Kim, B.-G. & Ahn, J.-H. Production of bioactive hydroxyflavones by using monooxygenase from *Saccharothrix espanaensis*. *J. Biotech.* **176**, 11–17, doi:10.1016/j.jbiotec.2014.02.002 (2014).
29. Jones, J. A. *et al.* Optimization of naringenin and *p*-coumaric acid hydroxylation using the native *E. coli* hydroxylase complex. *HpaBC. Biotechnol. Prog.* **32**, 21–25, doi:10.1002/btpr.2185 (2016).
30. Satoh, Y. *et al.* Engineering of L-tyrosine oxidation in *Escherichia coli* and microbial production of hydroxytyrosol. *Met. Eng.* **14**, 603–610, doi:10.1016/j.ymben.2012.08.002 (2012).
31. Jin, S. H. *et al.* Overexpression of glucosyltransferase UGT85A1 influences trans-zeatin homeostasis and trans-zeatin responses likely through O-glucosylation. *Planta* **237**, 991–999, doi:10.1007/s00425-012-1818-4 (2013).
32. Wang, L. *et al.* Comparing the acceptor promiscuity of a *Rosa hybrida* glucosyltransferase RhGT1 and an engineered microbial glucosyltransferase OleD(PSA) toward a small flavonoid library. *Carbohydr. Res.* **368**, 73–77, doi:10.1016/j.carres.2012.12.012 (2013).
33. Kim, B. G. *et al.* Cloning and expression of the isoflavone synthase gene (*IFS-Tp*) from *Trifolium pratense*. *Mol. Cells* **15**, 301–306 (2003).
34. Yoon, J.-A. *et al.* Production of a novel quercetin glycoside through metabolic engineering of *Escherichia coli*. *Appl. Env. Microbiol.* **78**, 4256–4262, doi:10.1128/AEM.00275-12 (2012).
35. Kim, B. G., Kim, H. J. & Ahn, J.-H. Production of bioactive flavonoid rhamnosides by expression of plant genes in *Escherichia coli*. *J. Agri. Food Chem.* **60**, 11143–11148, doi:10.1021/jf302123c (2012).
36. Kim, M. J., Kim, B.-G. & Ahn, J.-H. Biosynthesis of bioactive O-methylated flavonoids in *Escherichia coli*. *Appl. Microbiol. Biot* **97**, 7195–7204, doi:10.1007/s00253-013-5020-9 (2013).

Acknowledgements

This work was supported by a grant (NRF-2016R1A2B4014057), and Priority Research Centers Program (2009-0093824) through the National Research Foundation (NRF) funded by the Ministry of Education, Science and Technology, Republic of Korea.

Author Contributions

J.H.A. designed and initiated the experiments. D.C. and S.Y.K. conducted experiments. D.C., S.Y.K., and J.H.A. analyzed data and wrote manuscripts. All authors reviewed the manuscript.

Additional Information

Supplementary information accompanies this paper at doi:10.1038/s41598-017-02042-2

Competing Interests: The authors declare that they have no competing interests.

Publisher's note: Springer Nature remains neutral with regard to jurisdictional claims in published maps and institutional affiliations.



Open Access This article is licensed under a Creative Commons Attribution 4.0 International License, which permits use, sharing, adaptation, distribution and reproduction in any medium or format, as long as you give appropriate credit to the original author(s) and the source, provide a link to the Creative Commons license, and indicate if changes were made. The images or other third party material in this article are included in the article's Creative Commons license, unless indicated otherwise in a credit line to the material. If material is not included in the article's Creative Commons license and your intended use is not permitted by statutory regulation or exceeds the permitted use, you will need to obtain permission directly from the copyright holder. To view a copy of this license, visit <http://creativecommons.org/licenses/by/4.0/>.

© The Author(s) 2017